

γ -ray and ultra-high energy neutrino background suppression due to solar radiation

Shyam Balaji^{1,*}

¹*Laboratoire de Physique Théorique et Hautes Energies (LPTHE),
UMR 7589 CNRS & Sorbonne Université, 4 Place Jussieu, F-75252, Paris, France*

The Sun emits copious amounts of photons and neutrinos in an approximately spatially isotropic distribution. Diffuse γ -rays and ultra-high energy (UHE) neutrinos from extragalactic sources may subsequently interact and annihilate with the emitted solar photons and neutrinos respectively. This will in turn induce an anisotropy in the cosmic ray (CR) background due to attenuation of the γ -ray and UHE neutrino flux by the solar radiation. Measuring this reduction, therefore, presents a simple and powerful astrophysical probe of electroweak interactions. In this letter we compute such anisotropies, which at the Earth (Sun) can be at least $\simeq 5 \times 10^{-3}$ (1)% and $\simeq 1 \times 10^{-16}$ (2×10^{-14})% for TeV scale γ -rays and PeV scale UHE neutrinos respectively. We briefly discuss observational prospects for experiments such as the Fermi Gamma-Ray Space Telescope Large Area Telescope (Fermi LAT), High-Altitude Water Cherenkov (HAWC) detector, The Large High Altitude Air Shower Observatory (LHAASO), Cherenkov Telescope Array (CTA) and IceCube. The potential for measuring γ -ray attenuation at orbital locations of other active satellites such as the Parker Solar Probe and James Webb Space Telescope (JWST) is also explored.

I. INTRODUCTION

The extragalactic background is a superposition of all radiation sources, both individual and diffuse, from the edge of the Milky Way to the edge of the observable universe, and is thus expected to encode a wide range of phenomena [1, 2]. It is broadly comprised of electromagnetic radiation and neutrinos which have a characteristic energy density and spectrum. Contributions are guaranteed from established extragalactic γ -ray source classes such as active-galactic-nuclei (AGN), star-forming galaxies, and γ -ray bursts [3]. It provides a non-thermal perspective on the cosmos, which is also explored by the cosmic radio background, extragalactic cosmic rays (CRs), and neutrinos.

The electromagnetic component often referred to as the extragalactic background light (EBL) is the total integrated flux of all photon emission over cosmic time [4–6]. This EBL is dominated energetically by thermal relic radiation from the last scattering surface observed as the cosmic microwave background (CMB). Different physical processes characterize the EBL in each waveband: starlight in the optical, thermal dust emission in the infrared, and X-ray emission from AGN [7].

Similarly, for neutrinos, the high energy frontier is expected to be especially rich, with neutrinos from baryonic accelerators (γ -ray bursts, AGN, etc.) extending up to about $\simeq 100$ GeV [8]. At even higher energies, the ultra-high energy (UHE) regime will exhibit cosmogenic neutrinos and may even reveal the presence of topological defects, which could emit neutrinos via a variety of energy loss channels [8]. For sources far beyond the gamma ray horizon, neutrinos may be the only probe because, even at the highest energies, they propagate freely up to cosmological distances. The observation of UHE particles such as photons, ions, and neutrinos provides critical information on astrophysical systems as well as the mechanisms of

charged particle acceleration in these systems.

Since there is significant contamination from foregrounds, direct measurements of the EBL and neutrino background are difficult, necessitating the use of indirect observational or theoretical determinations to obtain an estimate of emitter populations [9]. Exotic contributions, such as those resulting from a possible connection between dark matter and Standard Model (SM) particles, may be present in addition to astrophysical emissions. This possibility was recently considered in Ref. [10]. Here the axion, a pseudo-Nambu-Goldstone boson initially proposed to solve the strong-CP problem—and axion-like particles (ALPs) were considered as a dark matter candidate. The ALP can decay into two photons based on the ALP-photon coupling and can contribute to the EBL. γ -ray attenuation is sensitive to multi-eV ALP decays through their contribution to the EBL [11–13]. Hence, additionally suppression of the γ -ray background due to the Sun as discussed in this work, could also affect constraints on dark matter candidates such as ALPs in the event of significantly improved flux resolution.

The interaction between the CMB and the cosmic neutrino backgrounds with γ -rays and UHE neutrinos and the subsequent CR anisotropies have been studied in detail [14–18]. Here, we will focus on a qualitatively different phenomena, computing instead the local anisotropy in the γ -ray and UHE neutrino background due to photon and neutrino emission from the Sun. A simple attempt at estimating the extinction of γ -rays due to sunlight was made in Ref. [19]. However the blackbody energy spectrum of the Sun was not included and the optical depth was estimated locally instead of being integrated over the entire region of the solar system where the sunlight and γ -rays are interacting. Additionally, the optical depth as a function of γ -ray energy or the observation angle from Earth relative to the Sun was not studied nor was the feasibility of probing the effect with γ -ray telescopes.

Here, we will include these effects and also consider the neutrino analogue whereby solar neutrinos annihilate with UHE antineutrinos or vice versa. We discuss the prospects for measuring the predicted γ -ray anisotropies with both space and ground-based experiments such as the Fermi Gamma-Ray Space Telescope Large Area Telescope (Fermi LAT), Cherenkov Telescope Array (CTA), the Large High Altitude Air Shower Observatory (LHAASO) as well as the High-Altitude Water Cherenkov (HAWC) experiment. We then discuss the possibility of measuring UHE neutrino anisotropies with the IceCube experiment. We also predict the expected attenuation at the Parker Solar Probe and James Webb Space Telescope (JWST) orbits and review the possibility of measuring EBL suppression due to the Sun at these locations in the future. Complete understanding of these anisotropies within the SM will enable constraints on beyond the SM models containing new states that could cause attenuation of the EBL or UHE neutrino background. In this letter, we will first outline the photon-photon and neutrino-antineutrino annihilation cross sections, then compute the optical depths and finally discuss experimental consequences. We will use natural units (where $\hbar = c = k_B = 1$).

II. ANNIHILATION PROCESSES

Cross sections

We will first consider the cross section for two photons annihilating into an electron-positron pair. For a γ -ray with energy E_γ , the annihilation cross section for the process $\gamma\gamma \rightarrow e^+e^-$ [20–22] with a solar photon γ_\odot of energy E_{γ_\odot} is given by

$$\sigma_{\gamma\gamma}(\beta) = \frac{3\sigma_T}{16}(1 - \beta^2) \times \left[2\beta(\beta^2 - 2) + (3 - \beta^4) \log\left(\frac{1 + \beta}{1 - \beta}\right) \right], \quad (1)$$

where $\sigma_T = \frac{8\pi}{3} \left(\frac{\alpha}{m_e}\right)^2 = 6.652 \times 10^{-25} \text{cm}^2$ is the Thomson scattering cross section, α is the fine structure constant, m_e is the electron mass and a dimensionless kinematic factor is defined $\beta = \sqrt{1 - E_{\text{th}}/E_\gamma}$. Where the threshold energy for electron-positron pair production is given by

$$E_{\text{th}} = \frac{2m_e^2}{E_{\gamma_\odot}(1 - \cos\theta)}. \quad (2)$$

In this expression θ refers to the scattering angle between the γ -ray and the solar photon. The threshold energy of the incident γ -ray for this process to occur when annihilating with a photon of energy $E_{\gamma_\odot} \simeq 0.5 \text{ eV}$ (like the effective temperature of the Sun) is at least $\simeq 0.5 \text{ TeV}$. Observing the bottom panel of Fig. 1, we see that the

scattering angle between the photons at which the cross section is maximised is highly dependent on the incident energy of the high energy γ -ray. Note that we will not consider higher order processes such as $\gamma\gamma \rightarrow e^+e^-e^+e^-$ since at high energy, the cross section approaches a relatively constant $6.5 \mu\text{b}$ [23] which is much lower than the leading order process unless $E_\gamma \gtrsim 10^8 \text{ TeV}$. Annihilation of photons into other final states such as $\mu^+\mu^-$ or $\pi^+\pi^-$ are subdominant at the scales of interest in this work.

For the neutrino channel, the resonant neutrino-antineutrino annihilation into a fermion-antifermion, $\nu\bar{\nu} \rightarrow Z^0 \rightarrow f\bar{f}$ occurs via the s -channel. It has Breit-Wigner shape and can be written [8, 14]

$$\sigma_{\nu\bar{\nu}}^R(p, k) = \frac{G_F \Gamma m_Z}{2\sqrt{2}k^2 p E_{\nu_\odot}} \int_{s_-}^{s_+} \frac{s(s - 2m_\nu^2)}{(s - m_Z^2)^2 + \xi s^2} ds, \quad (3)$$

where the Fermi constant is $G_F = 1.16637 \times 10^{-5} \text{GeV}^{-2}$ [24]. The light neutrino mass is set to $m_\nu = 0.08 \text{ eV}$ and we define a dimensionless ratio $\xi = \Gamma^2/m_Z^2$, where $\Gamma = 2.495 \text{ GeV}$ is the decay width of the Z boson with mass $m_Z = 91.1876 \text{ GeV}$ [24]. The UHE neutrino has 4-momentum $k^\mu = (E_\nu, \mathbf{k})$ while the solar neutrinos have $p^\mu = (E_{\nu_\odot}, \mathbf{p})$, hence it follows from the usual relativistic energy-momentum relation that $k = \sqrt{E_\nu^2 - m_\nu^2}$ and $p = \sqrt{E_{\nu_\odot}^2 - m_\nu^2}$. The centre-of-mass energy is $s = (p^\mu + k^\mu)^2 \simeq 2m_\nu^2 + 2\mathbf{k} \cdot (E_{\nu_\odot} \pm \mathbf{p})$ since $E_\nu \simeq k$ at high energy. Also, we have $\mathbf{k} \cdot \mathbf{p} = pk \cos\theta$. Hence the integration limits in Eq. (3) are defined $s_\pm = 2m_\nu^2 + 2k(E_{\nu_\odot} \pm p)$ corresponding to $\theta = 0$ and $\theta = \pi$ respectively.

We plot the resulting cross sections for photon-photon and resonant neutrino-antineutrino annihilation as a function of the incident cosmic ray particle energy in Fig. 1. We fix $E_{\gamma_\odot} = 0.5 \text{ eV}$ and $E_{\nu_\odot} = 0.53 \text{ MeV}$ respectively since these are the typical energies of photons and neutrinos being emitted from the Sun. The maximal cross section of $\sigma_{\gamma\gamma} \simeq 1.7 \times 10^5 \mu\text{b}$ for $\gamma\gamma$ occurs at $E_\gamma \simeq 1 \text{ TeV}$ while for $\nu\bar{\nu}$ it occurs at $E_\nu \simeq 4 \times 10^3 \text{ TeV}$ at $\sigma_{\nu\bar{\nu}}^R \simeq 4.8 \times 10^{-2} \mu\text{b}$.

There are also non-resonant contributions, which include several other channels with final states such as $\nu\nu \rightarrow \nu\bar{\nu}, l\bar{l}, WW, ZZ$ and Zh [25, 26], which we can approximate in total as in Ref. [15] with

$$\sigma_{\nu\bar{\nu}}^{NR} \simeq \frac{\sigma_{\nu\bar{\nu}}^{he}}{1 + E_r/E}, \quad (4)$$

where $E_r = \frac{m_Z^2}{2m_\nu}$ and $\sigma_{\nu\bar{\nu}}^{he} = 8.3 \times 10^{-4} \mu\text{b}$. This is significantly smaller than the resonant contribution below E_{th} so we can safely omit these contributions when considering UHE neutrino scattering in the regime of interest.

Optical depth

The radiation spectrum of the Sun can be approximated as a blackbody. The peak wavelength is around 500 nm .

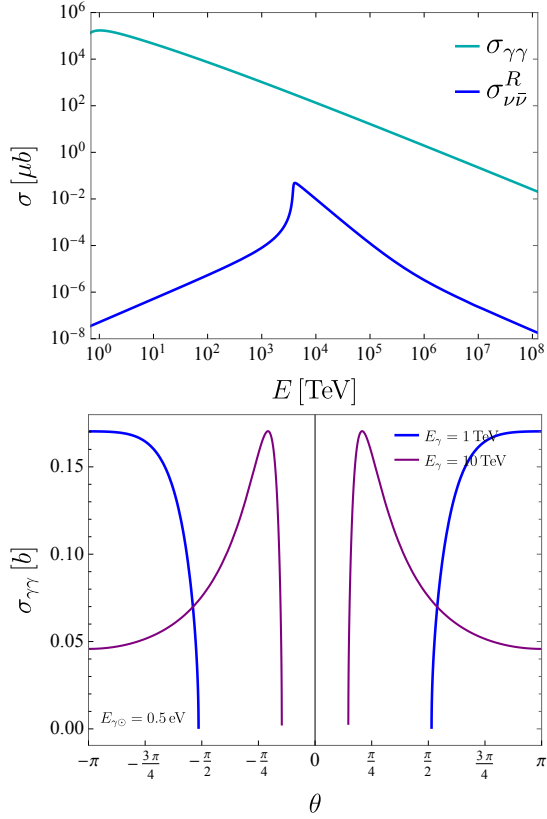


FIG. 1. In the top panel we show annihilation cross sections in units of μb (microbarns) for $\gamma\gamma$ (cyan) and resonant $\nu\bar{\nu}$ (blue) as function of the incident γ -ray or ultra-high energy neutrino respectively. We take $E_{\gamma\odot} = 0.5\text{eV}$ and $E_{\nu\odot} = 0.53\text{ MeV}$ since these are typical energies for photons and neutrinos being emitted by the Sun. In the bottom panel we show the dependence of the annihilation cross section in b (barns) on the incident angle between the scattering photons for two energies $E_\gamma = 1, 10\text{ TeV}$ while fixing $E_{\gamma\odot} = 0.5\text{ eV}$.

In natural units, we get the differential luminosity per unit energy to be [27]

$$\frac{dL_\odot}{dE_{\gamma\odot}} = 4\pi R_\odot^2 \frac{1}{2} \frac{4\pi}{(2\pi)^3} \frac{E_{\gamma\odot}^3}{e^{\frac{E_{\gamma\odot}}{T_{\text{eff}}}} - 1}, \quad (5)$$

where the prefactor of $1/2$ is to count only out going modes of the blackbody spectrum and the factors that follow to the right include the boson phase space and Bose-Einstein occupation number, $T_{\text{eff}} = 5780\text{ K}$ is the effective blackbody temperature of the Sun [28] and R_\odot is the solar radius. We can show a visual representation of the Sun-Earth-EBL(UHE ν) system in Fig. 2. There are non-thermal sources of electromagnetic radiation from the Sun, such as X-rays and γ -rays from solar flares, X-rays and radio waves from coronal mass ejections, Sun spots and solar prominences. However, since the spectrum is dominated in intensity by sunlight, we will focus on this moving forward. From here we can easily compute the differential photon number density per unit energy of the

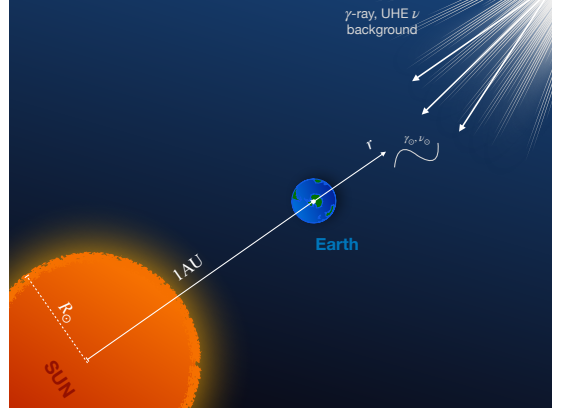


FIG. 2. Representation of coordinate system showing radial variable r where the extragalactic background photons and neutrinos interact with solar photons γ_\odot and neutrinos ν_\odot . r' is the position at which we want to compute observable optical depth.

Sun at a distance r from the solar core with

$$\frac{dn_{\gamma\odot}}{dE_{\gamma\odot}} = \frac{1}{4\pi r^2 E_{\gamma\odot}} \frac{dL_\odot}{dE_{\gamma\odot}}. \quad (6)$$

Note that there is an additional factor of c in the denominator which is omitted since $c = 1$ in natural units.

From here we may now turn our attention to calculating the optical depth associated with a CR photon travelling an arbitrary distance through a background of sunlight. The differential optical depth per unit energy is given

$$\frac{d\tau_\gamma}{dE_{\gamma\odot}} = \int_{r'}^\infty \frac{dn_{\gamma\odot}}{dE_{\gamma\odot}} \sigma_{\gamma\gamma}(E_\gamma, E_{\gamma\odot}, \theta) dr, \quad (7)$$

where we use (1) for $\sigma_{\gamma\gamma}$ and r' is the radial position at which we want to determine the γ -ray optical depth. Integrating over the solar photon energy to obtain the optical depth

$$\tau_\gamma = \int_{E_{\text{th}}}^\infty \frac{d\tau}{dE_{\gamma\odot}} dE_{\gamma\odot}. \quad (8)$$

We may also integrate the optical depth along the line-of-sight to obtain the dependence of the attenuation and the angle Θ , where $\Theta = 0$ is in the direction pointing directly towards the Sun from Earth (where the γ -ray background would be collinear with sunlight) and $\Theta = \pm\pi$ is pointing directly away from the Sun (where γ -rays would annihilate head on with sunlight). Note that θ is the scattering angle between incident photons, but Θ is the elongation angle at which observations from Earth would be performed. We may now plot the resulting optical depth due to the annihilation process as shown in Fig. 3 as a function of E_γ for a fixed angle of $\theta = \pm\pi$ (head-on collision) as well as the optical depth as a function of elongation angle relative to the Sun Θ for three representative energies $E_\gamma = [0.5, 1, 10]\text{ TeV}$. For observational purposes, (i) lower

E_γ values and (ii) larger angles of $|\Theta|$ (pointing away from the Sun) are more relevant since the (i) flux uncertainties associated with γ -rays in this regime are lower and (ii) TeV photons from the solar corona at small Θ would be a very large background, potentially obscuring the observation of γ -ray attenuation. For this reason, we will conservatively focus our discussion on attenuation for E_γ around a TeV at $\Theta = \pm\pi$. We also note that at small $|\Theta|$, there will be a large component of γ -rays resulting from a spatially extended component of the solar emission due to the inverse Compton scattering of CR electrons off solar photons [29], this would make small effects like the one considered here difficult to resolve. However, it should also be noted that such a contribution is focused within a few degrees of the Sun and becomes insignificant for elongation angles $|\Theta| \gtrsim 20^\circ$ [29]. We show the optical depth at the solar surface and at Earth (for $\Theta = \pm\pi$) in cyan and blue in the upper panel of Fig. 3 respectively. The maximal optical depth is around the threshold energy for the respective scattering angle. In the first case, the γ -ray photons must traverse through the sunlight till the surface of the Sun and in the second, the γ -ray must travel through a much lower number density of solar photons from beyond the Earth and Sun towards the Earth's surface. Unsurprisingly, of the two scenarios shown, the optical depth is maximised at the solar surface at around $\tau_\gamma = 1.1\%$ since the γ -rays interact with a much larger number density of photons in this region. At Earth, the optical depth is around $\tau_\gamma = 5.1 \times 10^{-3}\%$ for $E_\gamma = 0.5$ TeV at angles of $\Theta = \pm\pi$ as shown in the bottom panel of Fig. 3. In Ref. [19], the optical depth is estimated at 7% at the solar surface and $3.3 \times 10^{-2}\%$ at the Earth. In both cases, the estimate is noticeably different than what we obtain here. This is unsurprising since the energy distribution and radial dependence of the solar photons was not included or integrated over like here. We note that at elongation angles more focused around the Sun such as $\Theta = \pm\pi/4$, the optical depth as observed from Earth is unsurprisingly larger, by around a factor of 2 (relative to $\Theta = \pm\pi$) at $12 \times 10^{-3}\%$ for $E_\gamma = 0.5$ TeV. This is due to the larger density of solar photons the EBL γ -rays can interact with while travelling to Earth. However, as mentioned earlier, we will focus on the minimal optical depth at $\Theta = \pm\pi$ to be conservative in the remaining discussion. We also note that the γ -rays at 1 TeV have a very slightly larger optical depth than at 0.5 TeV for smaller elongation angles because of the threshold energy requirements set by the incident γ -ray energy and shape of the thermal spectrum of the Sun. For incident 10 TeV γ -rays, the attenuation is appreciably lower because as mentioned above, the maximal optical depth occurs around the threshold energy, and the number density of solar photons that satisfy the threshold energy corresponding to an incident γ -ray of 10 TeV is much lower (lying in the low energy tail of the thermal spectrum rather than around the peak). The attenuation is the

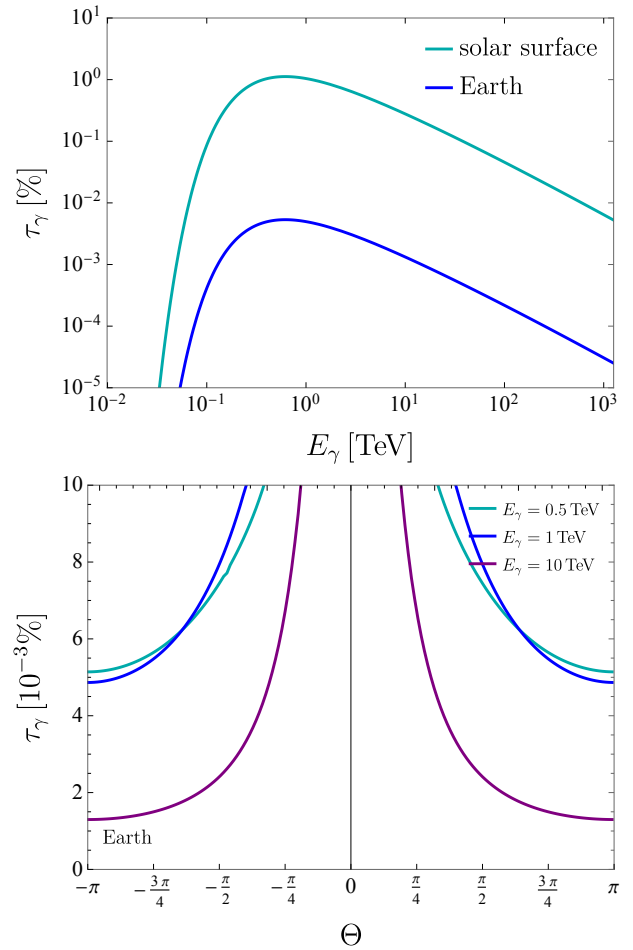


FIG. 3. In the top panel we show the percentage optical depth τ shown as a function of incident γ -ray energy in TeV. We show two scenarios, one is at the solar surface $r' = R_\odot$ (cyan) and the other is at Earth $r' = 1$ AU for elongation angle $\Theta = \pm\pi$ (blue). In both cases we take a scattering angle of $\theta = \pi$. In the bottom panel, we show percentage optical depth at Earth as a function of elongation angle Θ for three representative γ -ray energies, $E_\gamma = 0.5$ TeV (cyan), $E_\gamma = 1$ TeV (blue) and $E_\gamma = 10$ TeV (purple).

same for positive and negative Θ simply due to spherical symmetry of the process as observed at Earth.

For UHE neutrino annihilation, we first require the solar neutrino luminosity which can be approximated $L_{\nu\odot} = 0.023L_\odot$ where $L_\odot \simeq 4 \times 10^{33}$ erg/s is the total luminosity of the Sun [30]. We can approximate the neutrino number density at a distance r with

$$n_{\nu\odot}(r) = \frac{1}{4\pi r^2} \frac{L_{\nu\odot}}{\bar{E}_{\nu\odot}}, \quad (9)$$

taking $\bar{E}_{\nu\odot} = 0.53$ MeV as the average neutrino energy emitted by the Sun [30]. Now we may compute the approximate optical depth τ_ν , for a high energy neutrino

incident upon a solar neutrino

$$\tau_\nu = \int_{r'}^\infty n_{\nu\odot}(r) \sigma_{\nu\bar{\nu}} dr, \quad (10)$$

using the maximum resonant neutrino annihilation cross section (at 4 PeV from Fig. 1 and Eq. (3)), we get $\tau_\nu = 1 \times 10^{-16}\%$ at Earth and $2 \times 10^{-14}\%$ at the solar surface.

III. RESULTS AND DISCUSSION

Considering the Fermi LAT experiment [31], we see that the highest energy bin is 580-820 GeV. The reported intensity for this bin is $\simeq (9.7 \pm 6.0) \times 10^{-12} \text{ cm}^{-2} \text{ s}^{-1} \text{ sr}^{-1}$. If we consider that the intensity will be similar at 1 TeV, then we may multiply by the operating time of 1239 days, the angular coverage of 2.4 sr and an effective area of 8000 cm^2 [31] to get 20 γ -ray events. Multiplied with the optical depth at Earth from Section II, we get a reduction of $\simeq 3 \times 10^{-4}$ events. This is substantially below unity, so unless there is a factor of $\simeq 10^4$ improvement in event count, it's unlikely that Fermi LAT will be able to register any reduction in events. Furthermore, Fermi LAT has a flux uncertainty of $\gtrsim 60\%$ for γ -rays at such high energy this makes small effects of attenuation difficult to discern. The CTA is expected to become the largest and most sensitive observatory for very-high-energy γ -rays in the energy range from 20 GeV to more than 300 TeV. CTA will be capable of detecting γ -rays from extremely faint sources with unprecedented precision energy and angular resolution. CTA South is projected to have a peak differential energy flux sensitivity of around $E_\gamma^2 \frac{d\Phi}{dE_\gamma} \simeq 10^{-13} \text{ erg cm}^{-2} \text{ s}^{-1}$ with an energy resolution of about 5% and angular resolution of about 0.05° for 1 TeV photons [32]. For $E_\gamma = 1 \text{ TeV}$ and over a 4π angle, this corresponds to a differential flux sensitivity of $\simeq 5 \times 10^{-15} \text{ cm}^{-2} \text{ s}^{-1} \text{ sr}^{-1}$. This is $\gtrsim 3$ orders of magnitude better flux resolution than Fermi LAT. This suggests that one could hope for $\simeq 3 \times 10^{-2}\%$ γ -ray flux resolution at TeV scale. This would perhaps be the most promising way to test attenuation of γ -rays due to sunlight, which as we calculated earlier, is of the order of $10^{-3}\%$ at Earth. Therefore, CTA seems a hopeful candidate for achieving such a goal, however in this case, there could be systematic uncertainties associated with resolving such a tiny effect. This is because Imaging Air Cherenkov Telescopes (IACTs) like CTA have a narrow field of view and local systematics like atmospheric conditions. By combining different subsets of telescopes and pointing directions, CTA will be able to cover a large fraction of the Galactic plane with varying sensitivity and resolution. This could be effective for studying γ -ray attenuation at elongation angles away from the Sun. But, CTA will still be limited at probing elongation angles close to the Sun, as it will only record data at night.

The High Altitude Water Cherenkov Observatory (HAWC), completed in early 2015, has been used to observe the Crab Nebula at high significance across nearly the full spectrum of energies to which HAWC is sensitive. HAWC's sensitivity improves with the γ -ray energy. For $E_\gamma \gtrsim 1 \text{ TeV}$ the sensitivity is driven by the best background rejection and angular resolution ever achieved for a wide-field ground array. The total uncertainty at 1 TeV for HAWC in this measurement according to Ref. [33] appears to be around $\gtrsim 50\%$ in total flux at 1 TeV. In the more recent Crab Nebula measurement Ref. [34] by HAWC, the flux uncertainty is significantly improved at TeV scale, the flux is measured to be $(3.73 \pm 0.07) \times 10^{-11}$ and $(3.63 \pm 0.08) \times 10^{-11} \text{ TeV cm}^{-2} \text{ s}^{-1}$ respectively, depending on the energy resolution method used. This corresponds to a remarkable flux uncertainty of only $\simeq 2\%$.

LHAASO, can measure the energy and arrival direction of the γ -rays with high sensitivity and large effective area, and use them to probe the properties of the EBL, and thereby the solar attenuation effect described in this work. LHAASO has a larger effective area and a higher sensitivity for very-high-energy γ -rays than HAWC, especially in the multi-TeV and PeV range [35]. However, in both air shower detectors HAWC and LHAASO [36], their comparable flux resolution must improve significantly to probe solar attenuation of γ -rays at TeV scale.

More recently, an all-sky measurement of the anisotropy induced by cosmic rays travelling through our local interstellar medium and the interaction between the interstellar and heliospheric magnetic fields was performed [37]. The analysis was based on data collected by the HAWC and IceCube observatories in the northern and southern hemispheres at the same median primary particle energy of 10 TeV. In their sky maps, they determined the horizontal anisotropies to be $\simeq 10^{-2}\%$. The vertical direction of the anisotropy was also determined to be of the same order. However it is important to note that this is for all cosmic rays, including charged cosmic rays, not only γ -rays like we are interested here. In Ref. [38], they report an anisotropy of $8 \times 10^{-2}\%$ at 2 TeV and to $14 \times 10^{-2}\%$ at around 30 TeV, from cosmic rays once again. They state that TeV cosmic-ray anisotropy is primarily dipolar with amplitude $\simeq 0.1\%$, but also contains smaller scale structure with strength $10^{-2}\%$. Improvements can be made with larger instantaneous sky coverage and longer uninterrupted observation periods. This would enable reduction in statistical uncertainties below the signal strength and to resolve features with large angular extent. To probe the solar attenuation of γ -rays, it is necessary to obtain anisotropy maps and flux resolution of γ -rays at the same level of sensitivity as for cosmic rays described above. This would require significant improvement in experimental design and analysis. Such improvements in sensitivity would be a significant step forward in understanding the effects of sunlight on γ -ray propagation.

In Ref. [19], γ -ray attenuation is compared with the

dipole anisotropy measured by the Cosmic Background Explorer (COBE). This variation of $\simeq 0.12\%$ results from the Earth's orbital motion about the Solar system barycenter and strikingly lies between the EBL optical depths evaluated at the solar surface and Earth respectively [39]. However, it is also important to note that the CMB dipole anisotropy is at a significantly different energy scale and is not impacted by the same statistical and systematic uncertainties of the γ -ray sky at TeV scale.

The radial position of the Parker Solar Probe which orbits very close to the Sun's corona is around $9.86R_{\odot}$ from the solar centre [40]. Supposing EBL measurements could be performed in this orbit, excellent extraction of γ -ray suppression could be discerned. In the case of an orbit with similar radial position to the JWST, which is situated at the L2 Lagrange point, we would get a smaller EBL optical depth $\tau_{\gamma} \simeq 4.9 \times 10^{-3}\%$ at $E_{\gamma} = 1$ TeV at $\Theta = \pm\pi$. This is almost the same as on Earth, but if γ -rays are recorded at L2, the Earth's umbra would not interfere with the sunlight γ -ray interactions, which could provide a marginal improvement in the measurement.

For UHE neutrinos, in order to obtain optimistically large optical depths of $\tau_{\nu} = 1 \times 10^{-16}\%$ at Earth and $\tau_{\nu} = 2 \times 10^{-14}\%$ at the solar surface, we require energies of $E_{\nu} = 4$ PeV. It is unlikely that such anisotropies will be probed with experiments such as IceCube which only have $\mathcal{O}(1)$ event observations at PeV scale which is far too small to study such an anisotropy [41].

IV. CONCLUSION

We consider suppression of diffuse extragalactic γ -rays and ultra-high-energy (UHE) neutrinos due to annihilation upon interactions with large numbers of photons and neutrinos emitted locally by the Sun. The annihilation induces anisotropies in the extragalactic background light (EBL) at around a TeV with optical depths of at least $\tau_{\gamma} \simeq 1\%$ and $\tau_{\gamma} \simeq 5 \times 10^{-3}\%$ at the surface of the Sun and at Earth respectively. Such anisotropies are a direct prediction of Quantum Electrodynamics interactions and can only be probed with future γ -ray experiments such as Fermi LAT, HAWC, LHAASO and CTA, only if there is a significant improvement in the ability to measure flux and anisotropy resolution as well as reduction in systematic uncertainties.

HAWC has measured dipole anisotropies of $\simeq 10^{-2}\%$ due to cosmic rays travelling through the interstellar medium. We obtain an optical depth of $\simeq 2 \times 10^{-3}\%$ at Earth with elongation angle $\pm\pi$. At energies much higher, the annihilation cross section falls off appreciably as does the EBL flux. Measurements of the TeV EBL suppression at comparable elongation angles can be larger around the Parker Solar Probe orbit $\simeq 3.2 \times 10^{-2}\%$, while for telescopes at L2 such as the JWST, the anisotropy is smaller around $1.5 \times 10^{-3}\%$. New experiments at these

locations in the Solar System with γ -ray sensitivity could also probe EBL reduction. Experiments like HAWC and LHAASO would need to obtain sensitivities comparable to cosmic rays for the much smaller subset of γ -rays for this effect to be resolved. On the otherhand, CTA is expected to obtain flux resolution better than 0.1% for TeV γ -rays. This makes it an optimistic candidate to test the attenuation described in this work based on flux resolution, at elongation angles away from the Sun. However, even in this case, systematic uncertainties would need to be controlled to make the effect discernable. Hence we conclude that the comparisons in Ref. [19] of the γ -ray anisotropy with the CMB dipole anisotropy are overly idealized given the much greater experimental challenges associated with resolving the EBL at TeV scale described in the main body of this work.

In the case of ultra-high energy (UHE) neutrinos interacting with the solar neutrinos of average energy 0.53 MeV, we get much smaller optical depths. This is due to the smallness of the resonant and non-resonant contributions to the neutrino-antineutrino annihilation cross section. Even the most optimistic scenario can produce anisotropies of $2 \times 10^{-14}\%$ and $1 \times 10^{-16}\%$ for a PeV scale UHE neutrino scattering off 0.53 MeV solar neutrinos at the solar surface and at Earth respectively. Since experiments such as IceCube have only obtained a few PeV neutrino events, probing such a small anisotropy seems highly unrealistic with current experiments.

The result for diffuse γ -rays presents a theoretical opportunity to study fundamental photon-photon interactions between isotropic background photons and thermal photons produced by the Sun in our neighbourhood of the universe. Although it seems unrealistic to probe such an attenuation with current telescopes, this result is an important SM effect and can be amplified with beyond the SM contributions in future works. We do not study the effects on non-diffuse background contributions in detail, but the calculated optical depths may easily be applied to these scenarios as well.

V. ACKNOWLEDGEMENTS

SB is supported by funding from the European Union's Horizon 2020 research and innovation programme under grant agreement No. 101002846 (ERC CoG "CosmoChart") as well as support from the Initiative Physique des Infinis (IPI), a research training program of the IDEX SUPER at Sorbonne Université. SB would like to thank Maura E. Ramirez-Quezada, Yongchao Zhang and an anonymous referee for helpful discussions and feedback on the draft.

VI. APPENDIX

The closed form solution for the resonant neutrino-antineutrino annihilation cross section in Eq.(3) is given by

$$\sigma_{\nu\bar{\nu}}^R(p, k) = \frac{2\sqrt{2}G_F\Gamma m_Z}{2kE_{\nu\odot}} \left\{ \frac{1}{1+\xi} + \frac{m_Z^2}{4pk(1+\xi)^2} \log\left(\frac{f_+}{f_-}\right) + \frac{1-\xi}{(1+\xi)^2} \frac{m_Z^3}{4pk\Gamma} [\tan^{-1}(g_+) - \tan^{-1}(g_-)] \right\} \quad (11)$$

where $\xi = \Gamma^2/m_Z^2$ and

$$f_{\pm} = 4k^2(1+\xi)(E_{\nu\odot} \pm p)^2 - 4m_Z^2k(E_{\nu\odot} \pm p) + m_Z^4$$

$$g_{\pm} = \frac{2k(1+\xi)(E_{\nu\odot} \pm p) - m_Z^2}{\Gamma m_Z} \quad (12)$$

* sbalaji@lpthe.jussieu.fr

- [1] A. Lamastra, N. Menci, F. Fiore, L. A. Antonelli, S. Colafrancesco, D. Guetta, and A. Stamerra, *Astron. Astrophys.* **607**, A18 (2017), arXiv:1709.03497 [astro-ph.HE].
- [2] J. D. Finke, M. Ajello, A. Dominguez, A. Desai, D. H. Hartmann, V. S. Paliya, and A. Saldana-Lopez, (2022), arXiv:2210.01157 [astro-ph.GA].
- [3] E. R. Owen, A. K. H. Kong, and K.-G. Lee, *Monthly Notices of the Royal Astronomical Society* **513**, 2335 (2022).
- [4] A. Cooray, *Royal Society Open Science* **3**, 150555 (2016), arXiv:1602.03512 [astro-ph.CO].
- [5] K. K. Singh, K. K. Yadav, and P. J. Meintjes, *Astrophys. Space Sci.* **366**, 51 (2021), arXiv:2105.14293 [astro-ph.CO].
- [6] Q. Yan-kun and Z. Hou-dun, *Chin. Astron. Astrophys.* **46**, 42 (2022).
- [7] K. Mattila and P. Väisänen, *Contemp. Phys.* **60**, 23 (2019), arXiv:1905.08825 [astro-ph.GA].
- [8] C. Lunardini, E. Sabancilar, and L. Yang, *JCAP* **08**, 014 (2013), arXiv:1306.1808 [astro-ph.HE].
- [9] S. E. Caddy, L. R. Spitler, and S. C. Ellis, arXiv preprint arXiv:2205.16002 (2022).
- [10] J. L. Bernal, A. Caputo, G. Sato-Polito, J. Mirocha, and M. Kamionkowski, (2022), arXiv:2208.13794 [astro-ph.CO].
- [11] O. E. Kalashev, A. Kusenko, and E. Vitagliano, *Phys. Rev. D* **99**, 023002 (2019), arXiv:1808.05613 [hep-ph].
- [12] A. Korochkin, A. Neronov, and D. Semikoz, *Astron. Astrophys.* **633**, A74 (2020), arXiv:1906.12168 [astro-ph.HE].
- [13] A. Korochkin, A. Neronov, and D. Semikoz, *JCAP* **03**, 064 (2020), arXiv:1911.13291 [hep-ph].
- [14] J. C. D'Olivo, L. Nellen, S. Sahu, and V. Van Elewuyck, *Astropart. Phys.* **25**, 47 (2006), arXiv:astro-ph/0507333.
- [15] R. Ruffini, G. V. Vereshchagin, and S. S. Xue, *Astrophys. Space Sci.* **361**, 82 (2016), arXiv:1503.07749 [astro-ph.HE].
- [16] A. Franceschini, *Universe* **7**, 146 (2021).
- [17] A. Nikishov, *Zhur. Eksptl'. i Teoret. Fiz.* **41** (1961).
- [18] G. G. Fazio and F. W. Stecker, *Nature* **226**, 135 (1970).
- [19] A. Loeb, *Res. Notes AAS* **6**, 148 (2022), arXiv:2207.00671 [hep-ph].
- [20] G. Breit and J. A. Wheeler, *Phys. Rev.* **46**, 1087 (1934).
- [21] R. J. Gould and G. P. Schröder, *Phys. Rev.* **155**, 1404 (1967).
- [22] R. Ruffini, G. Vereshchagin, and S.-S. Xue, *Phys. Rept.* **487**, 1 (2010), arXiv:0910.0974 [astro-ph.HE].
- [23] R. Brown, K. Mikaelian, and R. Gould, *Astrophysical Letters* **14**, 203 (1973).
- [24] P. A. Zyla *et al.* (Particle Data Group), *PTEP* **2020**, 083C01 (2020).
- [25] E. Roulet, *Phys. Rev. D* **47**, 5247 (1993).
- [26] G. Barenboim, O. Mena Requejo, and C. Quigg, *Phys. Rev. D* **71**, 083002 (2005), arXiv:hep-ph/0412122.
- [27] A. Caputo, G. Raffelt, and E. Vitagliano, *Phys. Rev. D* **105**, 035022 (2022), arXiv:2109.03244 [hep-ph].
- [28] D. Lide, *CRC Handbook of Chemistry and Physics, 88th Edition* (Taylor & Francis, 2007).
- [29] A. A. Abdo *et al.* (Fermi-LAT), *Astrophys. J.* **734**, 116 (2011), arXiv:1104.2093 [astro-ph.HE].
- [30] A. Ianni, *Phys. Dark Univ.* **4**, 44 (2014).
- [31] M. Ackermann *et al.* (Fermi-LAT), *Astrophys. J.* **799**, 86 (2015), arXiv:1410.3696 [astro-ph.HE].
- [32] G. Maier, L. Arrabito, K. Bernlöhr, J. Bregeon, P. Cumani, T. Hassan, J. Hinton, and A. Moralejo (CTA Consortium), *PoS ICRC2019*, 733 (2020), arXiv:1907.08171 [astro-ph.IM].
- [33] A. U. Abeysekara *et al.*, *Astrophys. J.* **843**, 39 (2017), arXiv:1701.01778 [astro-ph.HE].
- [34] A. U. Abeysekara *et al.* (HAWC), *Astrophys. J.* **881**, 134 (2019), arXiv:1905.12518 [astro-ph.HE].
- [35] Z. Cao *et al.* (LHAASO), (2023), arXiv:2305.05372 [astro-ph.HE].
- [36] Z. Cao *et al.* (LHAASO), (2023), arXiv:2305.17030 [astro-ph.HE].
- [37] A. U. Abeysekara *et al.* (HAWC, IceCube), *Astrophys. J.* **871**, 96 (2019), arXiv:1812.05682 [astro-ph.HE].
- [38] A. U. Abeysekara *et al.*, *Astrophys. J.* **865**, 57 (2018), arXiv:1805.01847 [astro-ph.HE].
- [39] A. Kogut *et al.*, *Astrophys. J.* **419**, 1 (1993), arXiv:astro-ph/9312056.
- [40] M. E. Wiedenbeck *et al.*, *PoS ICRC2017*, 016 (2018).
- [41] M. G. Aartsen *et al.* (IceCube), *Phys. Rev. D* **98**, 062003 (2018), arXiv:1807.01820 [astro-ph.HE].